Acta Oceanol. Sin., 2023, Vol. 42, No. 7, P. 10–24
https://doi.org/10.1007/s13131-022-2077-2
http://www.aosocean.com
E-mail: ocean2@hyxb.org.cn

Sediment source-to-sink process variations of sandy-muddy transitional beaches and their morphological indications

Shaohua Zhao[1, 2, 3*], Feng Cai[1, 2, 3*], Hongshuai Qi[1, 2, 3], Jianhui Liu[1, 2, 3], Chao Cao[1, 2, 3], Gen Liu[1], Gang Lei[1, 2, 3]

[1] Laboratory of Ocean and Coast Geology, Third Institute of Oceanography, Ministry of Natural Resources, Xiamen 361005, China

[2] Key Laboratory of Marine Ecological Conservation and Restoration, Ministry of Natural Resources, Xiamen 361005, China

[3] Fujian Provincial Key Laboratory of Marine Ecological Conservation and Restoration, Xiamen 361005, China

Received 28 April 2022; accepted 22 June 2022

Abstract

The clay mineralogy of 28 sandy-muddy transitional beach (SMT-Beach) sediments and surrounding mountain river sediments along the coasts of southeastern China was systematically investigated to reveal the sediment source-to-sink process variations of such beaches and their morphological indications. The results show that the clay mineral assemblages of these SMT-Beaches mainly comprise of almost equal illite (~30%), kaolinite (~28%), chlorite (~22%), and smectite (~20%) contents. From the surrounding mountain rivers to the SMT-Beaches, clay mineral assemblages show distinct spatial changes characterized by a large decrease (~40%) in kaolinite, whereas the other three clay minerals present relative increases, especially clear for smectite. The muddy sediment sources of SMT-Beaches inferred from the clay mineralogy are mainly derived from nearby mountain rivers coupled with long-distance transport and penetration of the Changjiang River. The sandy sediments of these beaches are predominantly sourced from nearby mountain rivers, the weathering products of surrounding rocks in both mainland and island environments, and erosion of the "Old Red Sand" and "Red Soil Platform". However, the sandy sediment sources of the SMT-Beaches are largely reduced because of the remarkable decrease in the river fluvial supply associated with intensive human activities such as dam construction and coastal reclamation. Subsequently, the sandy sections of SMT-Beaches present clear erosion and have revealed by both time series remote sensing images and a compilation of published literature. In contrast, the muddy sediment supply of SMT-Beaches is temporarily stable and relatively constant, resulting in the landward migration of the mudflats with relative transgression or accumulation. These findings highlight that the natural evolution processes of SMT-Beaches have been greatly reshaped by intensive human activities.

Key words: sandy-muddy transitional beach, clay mineral, sediment source, human activity, fluvial discharge, morphological evolution

Citation: Zhao Shaohua, Cai Feng, Qi Hongshuai, Liu Jianhui, Cao Chao, Liu Gen, Lei Gang. 2023. Sediment source-to-sink process variations of sandy-muddy transitional beaches and their morphological indications. Acta Oceanologica Sinica, 42(7): 10–24, doi: 10.1007/s13131-022-2077-2

1 Introduction

Coastal zones have been heavily populated and developed and contains 40% of the world's population and 15 of the 20 megacities (population >10 million) (Luijendijk et al., 2018; Mentaschi et al., 2018 and references therein). Beaches, one of the most important natural resources in coastal zones, with 31% of the world's ice-free shorelines (Luijendijk et al., 2018), possess high value corresponding to their travel and leisure, disaster prevention and mitigation, and ecological maintenance services, providing the key for the rapid development of coastal tourism and cities worldwide (Stronge, 2005; Houston, 2013; Cai, 2015, 2019). In particular, numerous sandy beaches, accounting for only 27% of the long coast of China, have played an important role in coastal tourism development and ecological civilization construction in recent years (Zhao et al., 2014; MNRC, 2019–2021). However, such limited but valuable beach resources are suffering from extensive human activities coupled with global climate changes (Luijendijk et al., 2018; Mentaschi et al., 2018; Vousdoukas et al., 2020), and half of these beaches show erosion and retreat to varying degrees (Cai, 2019), resulting in great challenges and uncertainty in the development of coastal tourism and cities in China and ecological protection.

Sandy-muddy transitional beaches (SMT-Beaches) are a special type of beach between sandy beaches and tidal mudflats and are characterized by the exposed mudflats during low tidal periods (Short, 1991, 2006; Zhao et al., 2020a, b). Despite their lower attraction compared to sandy beaches, widely distributed SMT-Beaches are still valuable for potential tourism development, especially those in some highly developed coastal cities located in/surrounding moderate to large river estuaries that lack sandy

Foundation item: The National Natural Science Foundation of China under contract Nos 41930538, 42076211 and 42076058; the Scientific Research Foundation of the Third Institute of Oceanography, Ministry of Natural Resources under contract Nos 2022017 and 2019006; the China Postdoctoral Science Foundation under contract No. 2019M652248.
*Corresponding author, E-mail: zhaoshaohua@tio.org.cn; fcai800@126.com

beach tourism space (e.g., many cities located in and surrounding the Changjiang River Estuary in China; Jiang et al., 2014; Huang et al., 2016). Moreover, quite limited attention has been given to these SMT-Beaches, mainly due to the exposed mudflats leading to less attractive sightseeing during low-tide periods and the possibility of these beaches being rich in various pollutants, indicating their relatively low value for tourism development. Consequently, studies on SMT-Beach morphodynamics and sedimentation processes are rare (Anthony et al., 2002, 2015; Tamura et al., 2010; Morio et al., 2016; Chang et al., 2016, 2017; Zhao et al., 2020a, b), and the potential development and usage of these beaches are further constrained due to this limited knowledge.

Sediment source-to-sink transport processes are highly important for understanding SMT-Beach morphodynamics. These beaches are either stable or unstable due to the balance between the sediment budget and coastal dynamics (Wright and Short, 1984; Komar, 1998; Aagaard et al., 2013; Flemming, 2020 and references therein), while the sediment budget is closely correlated to variations in sediment supply capacities from source areas. SMT-Beaches are normally composed of narrow high-tidal sandy beaches and wide dissipative low-tidal mudflats and the boundaries between these zones are called sand-mud transition (SMT) (Morio et al., 2016; Chang et al., 2016, 2017; Zhao et al., 2020a, b). The relatively coarse sediments of the upper sandy section are normally derived from fluvial sediments of surrounding rivers and direct weathering products of nearby bedrock, whereas the fine sediments of the lower muddy section can be sourced from long-distance transport, or even be transported across the whole continental shelf and deep-sea basin, as inferred from clay mineralogy research (Xu et al., 2009; Liu et al., 2016; Zhao et al., 2018a). Previous studies have suggested that SMT-Beaches are widely distributed in river estuaries with high sediment supplies (Anthony et al., 2002, 2015; Pereira et al., 2011; Chang et al., 2016, 2017; Zhao et al., 2020b). Therefore, against the background of a dramatic decrease in global fluvial discharge (Syvitski et al., 2005; Walling, 2006; Milliman and Farnsworth, 2011), revealing the sediment sources of SMT-Beaches and their variations plays a key role in understanding SMT-Beach sedimentation and morphodynamic processes and their near-future evolution trends.

Large numbers of SMT-Beaches are well developed along the coast of China, especially along the western mesotidal to macrotidal coasts of the Taiwan Strait (TS) in southeastern China (SE China), and these beaches are characterized by circuitous coastlines, widespread semi-enclosed bays and mountain rivers, high sediment supplies, and contrasting hydrodynamic conditions (Huang et al., 2016; Zhao et al., 2020a, b; Guo et al., 2021; Fig. 1). Such coastal areas provide natural laboratories for studying and investigating the morphodynamic processes of SMT-Beaches. Simultaneously, some sandy beaches along the long coasts of China with high tourism value suffer from sea-level rise, sand mining, coastal reclamation, and industrial pollution discharge. The resultant decreased sand supply and weakened coastal hydrodynamics tend to lead to sandy beach retreat/erosion or even transformation into SMT-Beaches. Thus, investigations of SMT-Beaches could also provide substantial evidence to conquer this transformation by matching the actual demands of SMT-Beach nourishment. In particular, various studies on the mineral assemblage and geochemistry of river and sea surface sediments have revealed the main sources of sediments in the TS and adjacent areas and their transport processes and potential controlling factors (Liu et al., 2008a, b, 2016; Xu et al., 2009, 2012; Horng and Huh, 2011; Fang et al., 2012; Li et al., 2019, 2021). These previous achievements have provided basic information and are highly convenient for revealing the sediment source-to-sink processes of SMT-Beaches.

This study focuses on contrasting clay mineral compositions from various SMT-Beaches to those of surrounding mountain rivers along the coasts of SE China. In combination with published data on clay minerals and heavy minerals, the sediment source-to-sink processes of these SMT-Beaches are systematically analyzed. Then, the relatively long-term morphological responses of SMT-Beaches to the largely decreased sediment supply are revealed by time series remote sensing images and further confirmed by a compilation of published literature. The results of this study highlight that the natural processes of SMT-Beach evolution have been largely disturbed by intensive human activities.

2 Materials and methods

Mineral assemblage analysis is a powerful tool to reveal beach sediment sources, mainly when the source regions lie under contrasting bedrocks and/or prevailing climate, in which case chemical/physical weathering tend to product different clay/heavy mineral assemblages (Mehring and McBride, 2007; Hein et al., 2013; Parra et al., 2012; Carranza-Edwards et al., 2019; Morrone et al., 2020). To investigate the sediment sources of SMT-Beaches in the study area, totals of 64, 16, and 41 surface sediment samples were collected for clay mineral analysis from 28 SMT-Beaches, mudflats in adjacent bays, and nearby mountain rivers, respectively (Fig. 1, Table 1). Normally, according to their scales, 1–4 samples were obtained from each SMT-Beach and each bay, while 1–8 samples were obtained from each mountain river. Simultaneously, many previously published clay mineral data representing surface sediments and core-top sediments from the TS and surrounding mountain rivers were compiled to better synthesize the sediment sources of SMT-Beaches along the western coasts of the TS in SE China as well as the potential transport processes of these sediments (Xu et al., 2009, 2012, 2013, 2014; Chen et al., 2017; Liu et al., 2008b, 2016; Fang et al., 2018; Li et al., 2021; Zhao et al., 2021). By referring to published literature compilations on heavy minerals, geochemistry, and beach morphological variations (Xu, 1995, 1996; Hong and Chen, 2003; Fang et al., 2010, 2012; Ma et al., 2018; Gong, 2019; Zhao et al., 2020a, b; Guo et al., 2021), the sediment source-to-sink processes with changes are revealed, and their indications for SMT-Beach morphological variations are discussed.

The clay mineral compositions were identified by X-ray diffraction (XRD) performed on oriented mounts of decarbonated clay-sized (<2 μm) particles using a PANalytical X'Pert PRO diffractometer at the State Key Laboratory of Marine Geology (Tongji University). The detailed preparation of these oriented mounts was consistent with extensive previous studies conducted in and/or surrounding the study area (Liu et al., 2008b, 2016; Zhao et al., 2018a; Fang et al., 2018). All samples were measured in triplicate under the conditions of air-drying, ethylene-glycol solvation for 24 h, and heating at 490°C for 2 h. The identification and interpretation of clay minerals were mainly conducted on 3 XRD diagrams according to the (001) basal reflections, and then the proportion of each clay mineral species was semiquantitatively obtained using the MacDiff software. The peak areas of basal reflection stresses at 15–17 Å, 10 Å, and 7 Å were associated with smectite (including mixed layers), illite, and kaolinite/chlorite, respectively, while the ratio of the 3.57/3.54 Å peak areas was further used to determine the relative proportions of kaolinite

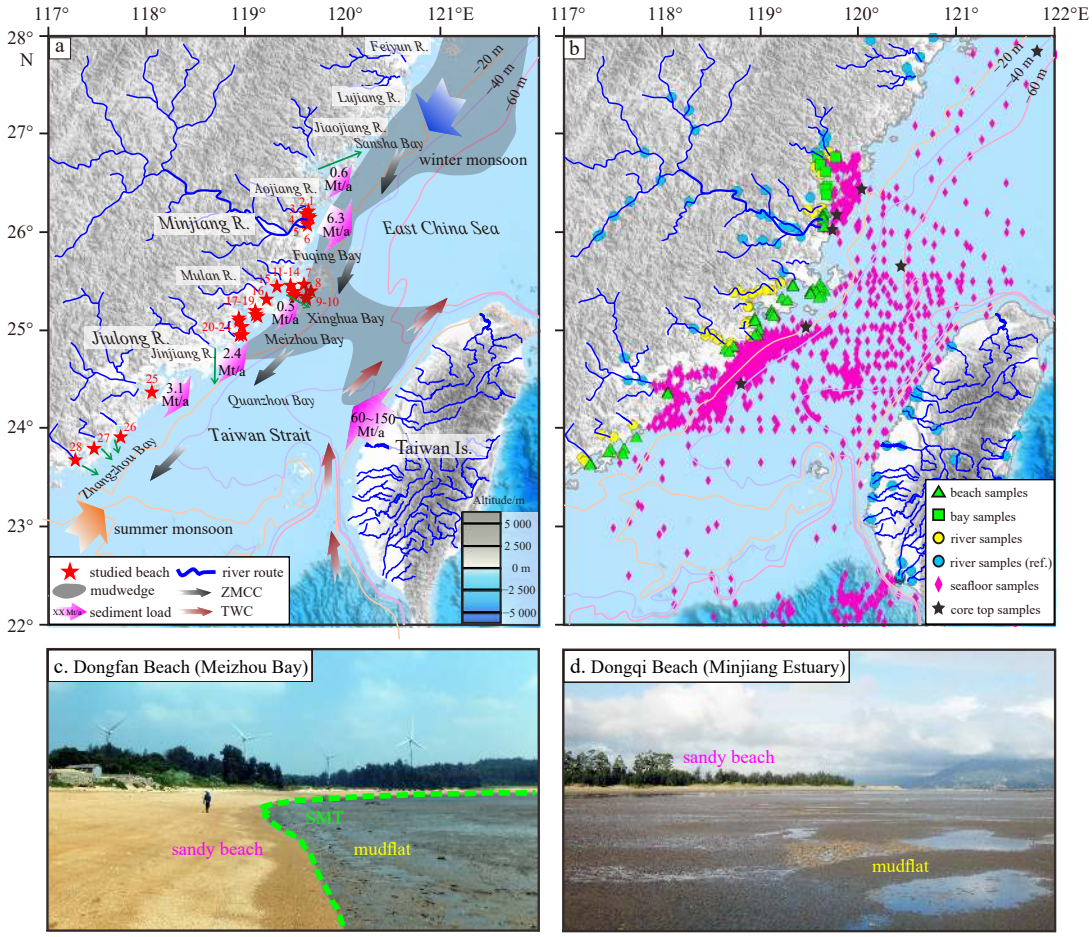

Fig. 1. Spatial distribution of the studied SMT-Beaches along the western coasts of the Taiwan Strait (TS) in southeastern China and the locations of the analyzed surface sediment samples. a. SMT-Beach distribution along the western coasts of the TS and surrounding fluvial drainage systems (redrawn from Zhao et al. (2020b)). The gradient magenta arrows marked with numbers represent the fluvial sediment discharge amounts (Mt/a) from the Chinese mainland and Taiwan Island (Milliman and Farnsworth, 2011). The translucent gray areas indicate the inner shelf mud wedge in the East China Sea (Xu et al., 2009). The red numbers show the locations of the SMT-Beaches, following the sequence in Table 1. b. Sample distribution of surface sediments. The green triangles and squares and yellow circles indicate the SMT-Beach sediments, bay samples, and river sediments collected in this study, respectively. The blue circles represent river sediment data surrounding the TS previously published by Xu et al. (2013), Liu et al. (2016), and Fang et al. (2018). The magenta diamonds indicate surface sediments in the TS reported by Xu et al. (2009, 2012, 2013), Liu et al. (2016), and Li et al. (2021), while the black stars indicate core-top sediments reported by Xu et al. (2014), Chen et al. (2017), Fang et al. (2018), and Zhao et al. (2021). c–d. The ground photo of typical SMT-Beaches. ZMCC: Zhe-Min Coastal Current; TWC: Taiwan Warm Current.

and chlorite. Considering the different calculation methods used to determine the relative clay mineral contents in previous studies, the weighing factors introduced by Biscaye (1965) were not used herein, and all the published data cited in this study were recalculated without the weighing factors. The accuracy of the semiquantitative evaluation of each clay mineral based upon the XRD method is ~5%. In addition, the illite crystallinity and illite chemical index were obtained from the half-height width of the 10 Å peak and the ratio of the 5 Å and 10 Å peak areas on the glycolated curve, respectively, providing two additional parameters to trace the sediment sources and their transport processess (Liu et al., 2008b, 2016).

3 Results

3.1 *Clay mineral assemblages of SMT-Beaches*

The clay mineral assemblages of 28 SMT-Beach sediments are mainly composed of illite (12%–38%), kaolinite (15%–66%), chlorite (10%–28%), and smectite (1%–32%), with average values of 30%, 28%, 22%, and 20%, respectively. The illite crystallinity and illite chemistry index values vary in the ranges of 0.159–0.224°Δ2θ (~0.182°Δ2θ) and 0.297–0.540 (~0.419), respectively. The clay mineral compositions at each SMT-Beach contrasted with those obtained from different river estuaries and/or bays, and are characterized by relatively obvious changes in both kaolinite and smectite (Figs 2 and 3a; Table 2). The clay mineral assemblages of the SMT-Beach sediments collected from the Minjiang Estuary, Xinghua Bay (including Fuqing Bay), Meizhou Bay, Jiulong Estuary, and Zhangzhou bays vary in the corresponding proportions of kaolinite-illite-chlorite-smectite, with 42%:26%:21%:10%, 21%:34%:25%:21%, 27%:32%:23%:19%, 40%:20%:23%:17%, and 39%:21%:21%:19%, respectively. Generally, the SMT-Beach sediments from the Minjiang Estuary, Jiulong Estuary, and Zhangzhou bays presented similar clay mineral assemblages with higher kaolinite contents, while those from both Xinghua Bay and Meizhou Bay show quite similar clay mineral

Table 1. Basic information of 28 SMT-Beaches along the southeastern China coast with sample amounts. The beach numbers follow the sequence shown in Fig. 1a. Length data of some SMT-Beaches are from Zhao et al. (2020b), while samples from the Minjiang River and Jiulong River are from Xu et al. (2013) and Liu et al. (2016)

Region	Rivers/samples	No.	Beach site	Latitude	Longitude	Length/m	Orientation/(°)	Samples
Minjiang Estuary	1. Minjiang R./21 2. Aojiang R./3	1	Xiaoao	26.209 207°N	119.653 316°E	350	116	3
		2	Changsha	26.194 579°N	119.625 588°E	1 350	107	2
		3	Zuokeng	26.167 555°N	119.629 629°E	640	65	4
		4	Longsha	26.160 987°N	119.638 562°E	430	63	2
		5	Guwei	26.080 202°N	119.649 282°E	1 920	86	2
		6	Dongqi	26.063 722°N	119.639 015°E	550	135	3
Fuqing Bay	1. Longjiang R./0	7	Yulou	25.482 611°N	119.603 250°E	300	70	2
		8	Nansha	25.409 777°N	119.651 725°E	170	146	1
Xinghua Bay	1. Mulan R./8 2. Shuangxia R./3	9	Xidou	25.348 457°N	119.594 570°E	150	2	1
		10	Shapu	25.430 283°N	119.529 880°E	350	59	1
		11	Laoshutou	25.404 283°N	119.572 018°E	140	8	1
		12	Dongchen	25.400 588°N	119.566 030°E	500	175	1
		13	Jiangxia	25.401 813°N	119.509 894°E	900	60	2
		14	Changshacun	25.381 171°N	119.509 949°E	460	168	3
		15	Jiangyin East	25.461 683°N	119.329 292°E	912	82	4
		16	Donggao	25.329 326°N	119.221 087°E	860	50	2
Meizhou Bay	1. Fengci R./2 2. Cangjiang R./2 3. Batou R./2 4. Houxu R./2	17	Dongfan	25.212 915°N	119.108 589°E	690	90	4
		18	Dongputou	25.173 904°N	119.112 948°E	810	50	2
		19	Jiangshan	25.160 736°N	119.135 017°E	340	100	2
		20	Wuli	25.137 955°N	118.937 994°E	1 430	64	3
		21	Zhengrong	25.109 103°N	118.944 836°E	440	155	2
		22	Houmenzai	25.021 598°N	118.984 060°E	700	330	2
		23	Lianfeng	24.962 353°N	118.966 688°E	700	15	3
		24	Cunbian	24.959 330°N	118.938 965°E	390	155	2
Jiulong Estuary	1. Jiulong R./3	25	Nantaiwu	24.375 105°N	118.051 810°E	1 730	80	4
Zhangzhou bays	1. Lujiang R./1	26	Liu'ao West	23.926 829°N	117.736 837°E	1 200	240	1
	2. Zhangjiang R./2	27	Lieyu	23.808 034°N	117.469 858°E	1 650	75	2
	3. Dongjiang R./3	28	Tiancuo	23.661 567°N	117.264 838°E	1 910	70	3

Note: 4 and 3 surface samples were collected from the mudflats of Sansha Bay and Quanzhou Bay, respectively. However, they are not presented in the table because there are no samples from SMT-Beaches. In addition, 2, 1, and 1 surface samples were obtained from the Jiaojiang River, Bianping River, and Feiluan River surrounding the Sansha Bay, respectively, while 5, 2, and 2 surface samples are collected from Jinjiang River, Luoyang River, and Zhetan Rive surrounding the Quanzhou Bay, respectively.

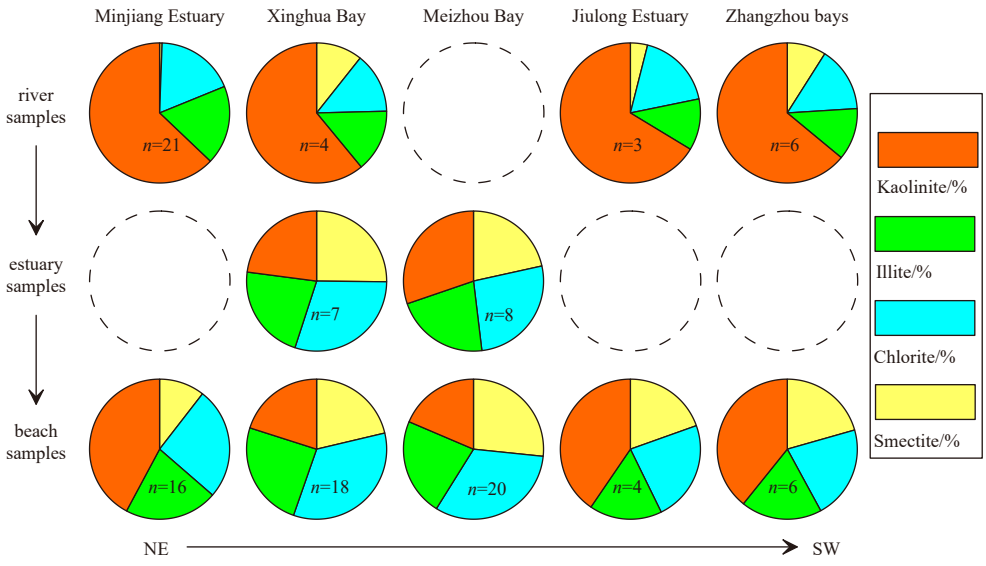

Fig. 2. Spatial variations in the clay mineral assemblages of surface sediments from rivers to river estuaries, and then to SMT-Beaches. The clay mineral data of surface sediments from the Minjiang River and Jiulong River are after Xu et al. (2013) and Liu et al. (2016).

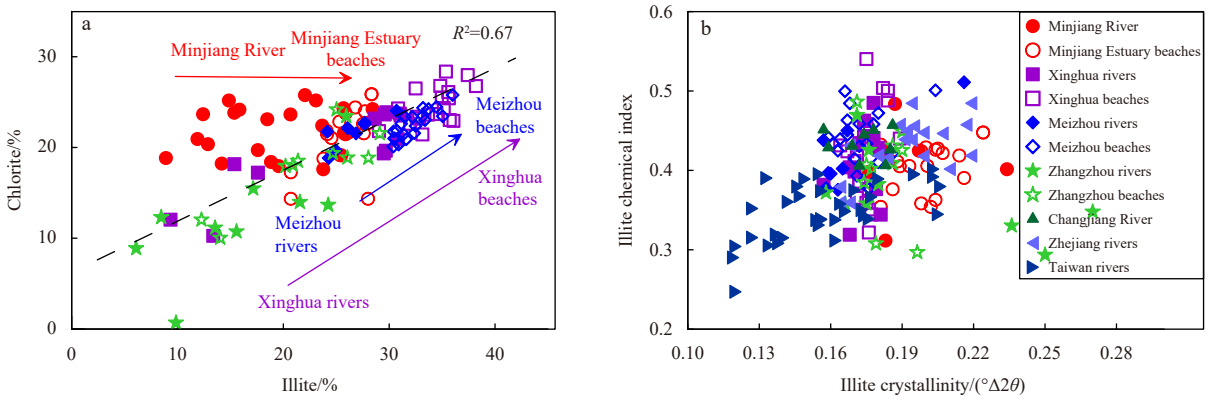

Fig. 3. Illite and chlorite features of SMT-Beach surface sediments and their comparison with surrounding rivers. a. Linear correlation between the illite and chlorite contents of SMT-Beach sediments and surrounding river samples. b. Illite crystallinity plots with the illite chemical index of the SMT-Beach sediments and their potential sources. The Changjiang River and Zhejiang rivers data are after Fang et al. (2018) and Liu et al. (2016), and the Fujian rivers data are after Xu et al. (2013) and Liu et al. (2016).

Table 2. Clay mineral assemblages of surface sediments from SMT-Beaches and their comparison with those from surrounding mountain rivers

Region	Location numbers	Smectite/%	Illite/%	Chlorite/%	Kaolinite/%	Illite crystallinity/(°Δ2θ)	Illite chemical index
Sansha Bay	estuary n=8	13 (2–19)	32 (16–38)	26 (21–30)	29 (18–61)	0.177 (0.163–0.199)	0.409 (0.360–0.476)
	mudflat n=4	24 (13–32)	34 (31–37)	23 (20–28)	19 (15–25)	0.178 (0.164–0.184)	0.404 (0.386–0.445)
Minjiang Estuary	river n=21	1 (0–5)	18 (9–26)	18 (0–25)	62 (50–83)	0.201 (0.182–0.234)	0.437 (0.401–0.484)
	beach n=16	10 (1–17)	26 (21–28)	21 (14–26)	42 (33–61)	0.201 (0.181–0.224)	0.406 (0.354–0.448)
Xinghua Bay	river n=4	11 (0–27)	14 (9–18)	14 (12–18)	61 (49–78)	0.174 (0.168–0.178)	0.420 (0.319–0.485)
	estuary n=7	25 (21–30)	30 (29–31)	22 (19–24)	23 (21–26)	0.173 (0.157–0.181)	0.399 (0.344–0.463)
	beach n=18	22 (14–27)	34 (29–38)	24 (21–28)	20 (15–27)	0.175 (0.164–0.189)	0.420 (0.322–0.540)
Meizhou Bay	estuary n=8	22 (17–27)	27 (24–31)	22 (19–24)	30 (24–36)	0.168 (0.157–0.216)	0.418 (0.376–0.511)
	beach n=20	27 (19–32)	32 (30–36)	23 (20–26)	19 (17–22)	0.173 (0.159–0.204)	0.439 (0.377–0.501)
Quanzhou Bay	river n=4	1 (0–2)	12 (11–13)	12 (11–14)	75 (73–78)	0.195 (0.179–0.213)	0.394 (0.353–0.421)
	estuary n=7	13 (2–27)	23 (16–29)	19 (13–22)	45 (28–51)	0.175 (0.158–0.194)	0.424 (0.396–0.472)
Jiulong Estuary	river n=3	4 (1–9)	18 (14–24)	12 (11–14)	67 (53–74)	0.171 (0.158–0.180)	0.393 (0.372–0.426)
	beach n=4	20 (10–24)	23 (14–28)	17 (10–19)	40 (24–47)	0.184 (0.174–0.196)	0.349 (0.297–0.409)
Zhangzhou bays	river n=6	9 (0–25)	15 (6–26)	12 (1–23)	64 (35–85)	0.211 (0.171–0.270)	0.360 (0.293–0.470)
	beach n=6	21 (14–30)	21 (12–29)	19 (12–24)	39 (25–64)	0.182 (0.171–0.190)	0.433 (0.402–0.486)

Note: All clay mineral data shown in this table are from this study except those of surface sediments from the Minjiang River and Jiulong River, which are after Xu et al. (2013), Liu et al. (2016), and Fang et al. (2018).

compositions with higher illite contents compared to the other three equal clay mineral species. In addition, the average illite crystallinity of the SMT-Beach sediments sampled from the Minjiang Estuary, Xinghua Bay, Meizhou Bay, Jiulong Estuary, and Zhangzhou bays are 0.201°Δ2θ, 0.175°Δ2θ, 0.173°Δ2θ, 184°Δ2θ, and 0.182°Δ2θ, while the average illite chemical index of SMT-Beach sediments sampled from the five regions are 0.406, 0.420, 0.439, 0.349, and 0.433, respectively (Table 2).

3.2 *Clay mineral compositions of surrounding river samples*

The clay mineral assemblages of the surface sediments collected from surrounding mountain rivers are mainly composed of dominant kaolinite (~49%), moderate illite (~22%) and chlorite (~19%), with minor smectite (~10%), according to the 41 samples analyzed in this study coupled with 30 published data points. The average illite crystallinity and the average illite chemical index of these sediments are 0.181°Δ2θ and 0.404, respectively. The kaolinite-illite-chlorite-smectite proportions in the surface sediments sampled from mountain rivers surrounding the Minjiang Estuary, Xinghua Bay, Jiulong Estuary, and Zhangzhou bays are 62%:18%:18%:1%, 61%:14%:14%:11%, 67%:18%:12%:4%, and 64%:15%:12%:9%, respectively (Fig. 2, Table 2). The average illite crystallinity of river sediments from these four regions are 0.201°Δ2θ, 0.174°Δ2θ, 171°Δ2θ, and 0.211°Δ2θ, while the average illite chemical indices of these sediments are 0.437, 0.420, 0.393, and 0.360, respectively. In addition, the surface sediments obtained from river estuaries in Sansha Bay, Xinghua Bay, and Meizhou Bay feature clay mineral assemblages with kaolinite-illite-chlorite-smectite proportions of 29%:32%:26%:13%, 23%:30%:22%:23%, and 30%:27%:22%:22%, respectively, with average illite crystallinity and the average illite chemical indices of 0.177°Δ2θ and 0.409, 0.173°Δ2θ and 0.399, and 0.168°Δ2θ and 0.418, respectively (Table 2).

4 Discussion

4.1 *Spatial variations in the clay mineral assemblages of surface sediments*

The clay mineral assemblages of surface sediments determined herein indicate obvious spatial discrepancies from the upper-middle river drainage basin to the river mouths and then to the SMT-Beaches in and surrounding the estuary regions, featur-

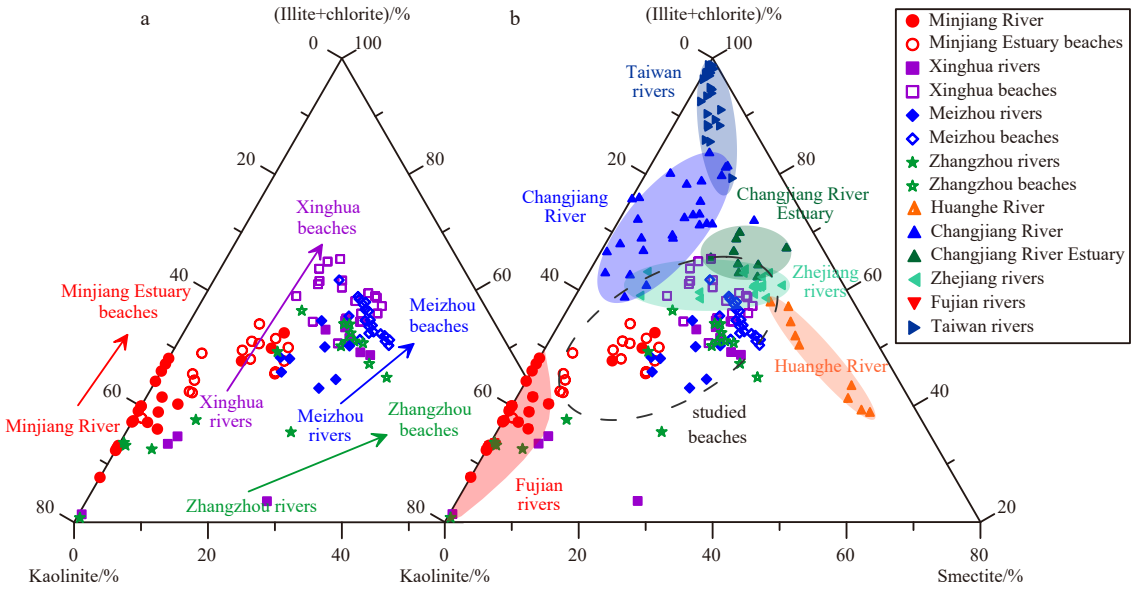

Fig. 4. Ternary diagram plotting the clay mineral assemblages of SMT-Beaches and their comparison with the potential source rivers. Fujian rivers data are from Xu et al. (2013), Liu et al. (2016), and Fang et al. (2018); Zhejiang rivers data are from Liu et al. (2016) and Fang et al. (2018); Taiwan rivers data are from Liu et al. (2008b, 2016); the Changjiang River and the Changjiang River Estuary data are from Xu et al. (2009), He et al. (2013), Fang et al. (2018), and Zhao et al. (2018b); and the Huanghe River data are from Yang (1988) and Yang et al. (2003).

ing largely decreased kaolinite contents coupled with relatively increased illite and smectite contents (Figs 2, 3a and 4a; Table 2). Higher kaolinite (>60%) and lower smectite (<10%) contents are observed in the surface sediments of the upper-to-middle river basin, whereas the kaolinite contents largely decrease by a value of ~30% in the river estuaries, coinciding with synchronous ~10% increases in both the illite and smectite contents, which are particularly clear in Xinghua Bay. Simultaneously, from the river estuaries to the adjacent SMT-Beaches, the kaolinite contents still decrease, while both the illite and smectite contents increase unceasingly. However, there is no clear spatial discrepancy in either the illite crystallinity or the illite chemical index (Fig. 3b, Table 2). In addition, the analogous illite and chlorite present a good linear correlation (R^2=0.67, Fig. 3a), which is consistent with previous studies on clay mineralogy in the TS, the adjacent East China Sea and the South China Sea (Liu et al., 2008b, 2016; Fang et al., 2018; Zhao et al., 2021), indicating their similar production processes from physical erosion (Wilson, 2004).

The clear spatial variations in the clay mineral assemblages of surface sediments from river basins to river estuaries and then to SMT-Beaches are mainly correlated with the sediment sources, differential settling, and tidal power. In the SE China drainage basin, the bedrock experiences long-term strong and thorough chemical weathering due to the low-relief and stable morphology coupled with stable tectonic settings and the warm and humid climatic conditions of the East Asian monsoon. In this case, widespread granitic rocks and sedimentary rocks preferentially produce and accumulate high contents of kaolinite (Liu et al., 2007b, 2016). Moreover, the strong monsoonal rainfall and scouring allow both illite and chlorite to form from the physical weathering of bedrock in the study area. When these clay minerals enter a river estuary or marine environment, different clay minerals can differentially settle due to their contrasting grain-sizes and chemical features, characterized by a large decrease in the kaolinite content and a relative increase in the smectite content (Gibbs, 1977; Liu et al., 2016). Kaolinite possesses large grain-sizes with a range of 0.5–8.0 μm and flocculates and settles quickly in alkaline seawater, probably explaining the 30% decrease in kaolinite observed from the drainage basin to the river estuary. By comparison, smectite with the relatively small grain-size (<1.0 μm) represents the fast chemical weathering production of andesitic-basaltic volcanic rocks (Wilson, 2004), and these sediments can be transported over long distances and favor deposition in calm environments. In further consideration of the limited distribution of volcanic rocks, the presence of smectite in the surface sediments of mountain rivers in the study area is quite rare (Xu et al., 2013; Liu et al., 2016; Fang et al., 2018). Consequently, the smectite increases from the upper-to-middle river basins to the SMT-Beaches in the river estuary could have other sources, in addition to those deduced from the differential settling effect. Furthermore, the estuaries of these mountain rivers are under strong macrotidal control, i.e., the average tide is larger than 4 m in the estuaries of the Minjiang River, Mulan River, and Jinjiang River, and the average spring tide is larger than 7 m (Zheng et al., 1982; Fu et al., 2013). Especially during flooding periods, large amounts of seawater enter the narrow river channels, delivering certain abundances of sediments and mixing with the fluvial sediments, thereby increasing the spatial diversity of clay mineralogy along the river routes and coastal areas.

4.2 *Source-to-sink processes of SMT-Beach sediments*

4.2.1 *Mud sources and transport processes*

According to the spatial distribution of clay minerals from rivers to SMT-Beaches described above, the muddy sediments of SMT-Beaches not only originate from nearby mountain rivers but can also be derived from other source areas through long-distance transport. Previous studies have reported that TS sediments mainly originate from numerous rivers on the Chinese mainland and Taiwan Island (Liu et al., 2008a, 2016, 2018; Xu et al., 2009, 2013; Horng and Huh, 2011; Fang et al., 2012; Li et al.,

2019, 2021). In further consideration of the clay mineralogy representing different regions, the Chinese mainland can be divided into three source subregions, i.e., the Changjiang River, Zhejiang rivers, and Fujian rivers, as suggested by Zhao et al. (2021). Sediments sourced from the Changjiang River are characterized by major illite (~45%), moderate chlorite (~28%) and kaolinite (~22%), and minor smectite (~6%) contents (He et al., 2013; Zhao et al., 2018b); Fujian rivers provide principal kaolinite (~61%) with moderate illite (~18%) and chlorite (~19%) contents; Zhejiang rivers contribute relatively equal illite (~37%), chlorite (~24%), smectite (~23%), and kaolinite (~16%) contents; and Taiwan rivers deliver predominant illite (~56%) and chlorite (~36%) contents (Liu et al., 2008b, 2016; Fang et al., 2018). Generally, the sediment sources from the Taiwan and Fujian rivers are recognizable due to their contrasting clay mineral assemblages, while the Changjiang River and Zhejiang rivers supply similar clay mineral contents (Fig. 4b).

A ternary diagram plotting the clay mineral assemblages of SMT-Beaches and the above four potential source areas indicates that the muddy sediments of these SMT-Beaches have obvious multiple sources (Fig. 4b). The analogous illite and chlorite contents plot at one end-member in the ternary diagram, while the smectite and kaolinite contents are recognized as the other two end-members. The clay mineral data representing all these potential source areas are plotted on the line between the kaolinite end-member and illite + chlorite end-member; the Fujian and Taiwan rivers are located on the two other sides, while both Zhejiang rivers and the Changjiang River are plotted in the central areas. All the clay mineral data of SMT-Beaches mainly fall in the areas constrained by the Fujian rivers, Zhejiang rivers, and the Changjiang River, indicating that the muddy sediment sources of the SMT-Beaches may mostly originate from these three sources.

To further determine the muddy sediment sources of SMT-Beaches, the clay mineral data obtained in this study were coupled with more than 1 000 available samples retrieved from the TS and surrounding areas (including some core-top samples, Xu et al., 2009, 2012, 2013, 2014; Chen et al., 2017; Liu et al., 2016; Fang et al., 2018; Li et al., 2021; Zhao et al., 2021; Fig. 1b) to reveal the spatial distribution of the TS clay minerals (Fig. 5). Both kaolinite and smectite are mainly distributed in the western TS and present quite similar spatial distributions, with especially high contents in the river estuaries and semi-enclosed bays (Figs 5a, c). In contrast, the spatial distribution of high illite and chlorite contents reflects the middle-to-eastern TS surrounding the Taiwan Island, with relatively low values in the western TS (Fig. 5b). Simultaneously, this result is also well correlated with the estimated TS clay contributions from each source region. Using the linear separation method for illite crystallinity proposed by Liu et al. (2008b, 2016) and applied in a sedimentary study in the East China Sea by Fang et al. (2018), the clay contributions of the TS muddy sediments from the Fujian rivers, Taiwan rivers, and Changjiang River (including the Zhejiang rivers) were obtained (Fig. 6). Taiwan rivers contribute most clay minerals to the middle-to-eastern TS (Fig. 6c), while the Fujian rivers and Changjiang River provide the most clay minerals along the coasts of the western TS (Figs 6a, d), implying potentially strong effects on the SMT-Beach morphology.

In view of the spatial distribution of both clay minerals and their contributions from various sources and the corresponding sediment supply capacity (Figs 5 and 6), the clay minerals of SMT-Beaches mainly originate from Fujian rivers and the Changjiang River, with a minor proportion from Zhejiang rivers. This observation indicates obvious provenance control and long-distance transport by oceanic currents, which are especially clear in the Minjiang Estuary, Xinghua Bay, and Meizhou Bay. Fujian rivers contribute 17–20 Mt/a fluvial sediments with high contents of kaolinite to the TS (Xu et al., 2013; Jia et al., 2018). In particular, most of these sediments are trapped in river estuaries due to differential settling and hindered by the strong Zhe-Min Coastal Current (ZMCC) and/or Taiwan Warm Current (TWC) (Ma et al., 2018; Li et al., 2019; Fig. 1), providing an important source for SMT-Beach muddy sediments. By comparison, the Changjiang River could be another significant source for SMT-Beach muddy sediments due to its larger sediment supply (470 Mt/a and 130 Mt/a for annual sediment discharge before and after the Three Gorges Dam, Milliman and Farnsworth, 2011; MWRC, 2002–2020; Dai et al., 2018; Dai, 2021) than those of both Fujian rivers and Zhejiang rivers (~13 Mt/a, Jia et al., 2018). Approximately 30% of these sediments can be transported southward by the ZMCC after a special process characterized by "deposition in summer and transport in winter" (Yang et al., 1992, Liu et al., 2018; Jia et al., 2018). These long-distance transported sediments, with high illite crystallinity and chemical index and high illite and chlorite contents, disperse in the inner shelf of the East China Sea and penetrate the river estuaries and bays along their transport route (Figs 1a, 5d, 6a, and 6b; Xu et al., 2009; He et al., 2013; Zhao et al., 2018b), even reaching the middle-to-southern areas of the TS (Liu et al., 2007a). Simultaneously, some proportion of Zhejiang river-sourced sediments are also transported southward by the ZMCC and mixed with the Changjiang River-sourced sediments, contributing some portion of muddy sediments to the SMT-Beaches. It must be pointed out that Taiwan rivers with large fluvial discharge (60–150 Mt/a) were found to provide limited muddy sediments for SMT-Beaches in this study, mainly due to the constrained sediments in the middle-to-eastern TS by the ZMCC and the TWC (Xu et al., 2009, 2013; Figs 5b and 6d).

Additionally, the high smectite contents of SMT-Beaches along these estuaries and bays are mainly derived from northern regions, although this is still under debate. All rivers surrounding the TS and the Changjiang River contribute limited smectite (Fig. 4), while Zhejiang river-sourced sediments have relatively high smectite contents but small fluvial discharges of only ~13 Mt/a (Jia et al., 2018; Fig. 5a), making it difficult for these rivers to disperse and distribute smectite throughout the whole inner shelf of the East China Sea. In contrast, a recent study suggested that the widespread smectite in the mud wedge of the East China Sea could also partly originate from the fluvial and/or resuspended sediments of the Huanghe River and its abandoned delta (Zhao et al., 2018b). The Huanghe River delivers the largest sediment amount into the ocean worldwide (~1 100 Mt/a, Milliman and Farnsworth, 2011), with a much higher smectite content (~40%) than those of the Changjiang River and Zhejiang rivers (Yang, 1988; Yang et al., 2003). Then, the resuspended sediments of the old Huanghe River delta are carried by southward coastal currents associated with the winter monsoon and arrive at the Changjiang River Estuary. These sediments are then mixed with the Changjiang River-sourced clay minerals and are further transported by the ZMCC over long distances, penetrating into river estuaries and semi-enclosed bays along the western coasts of the TS under differential settling (Xu, 1985; Zhao et al., 2018b; Fig. 5a) and contributing a certain amount of clay minerals to SMT-Beaches. In addition, the smectite sampled in SMT-Beaches in the southern Zhangzhou bays may be derived from fast weathering processes of nearby volcanic rocks in South China delivered by northward coastal currents in summer (Liu et

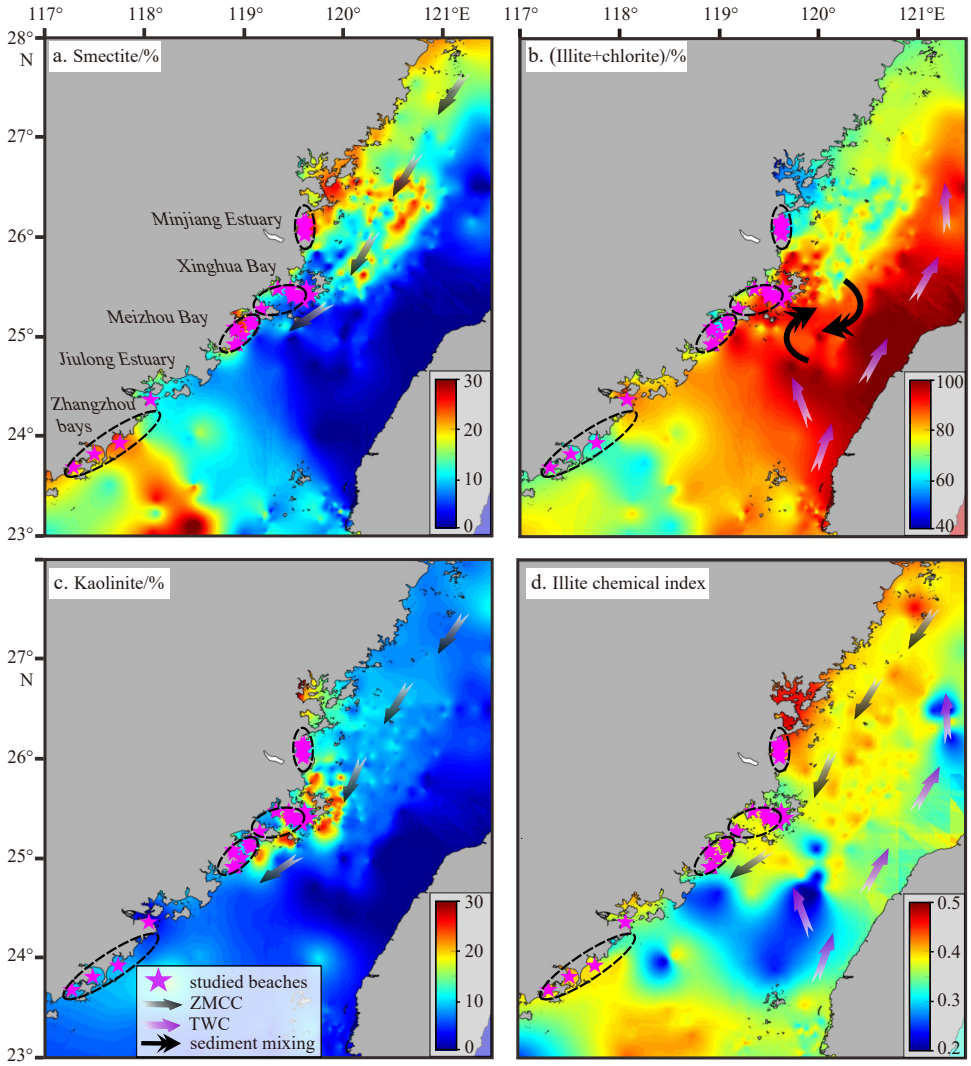

Fig. 5. Spatial distribution of clay minerals in the Taiwan Strait and their sediment transport process indication. a–d present the spatial distributions of smectite, illite + chlorite, kaolinite, and the illite chemical index, respectively. Note: the red areas indicate high values, while the blue areas imply low values, although the scale of each subfigure is different. ZMCC: Zhe-Min Coastal Current; TWC: Taiwan Warm Current.

al., 2019). To summarize, the smectite sources of SMT-Beaches in the study areas are still unclear and thus need further investigation with new methods to better constrain this issue. Nevertheless, most smectite in the analyzed SMT-Beaches is mainly transported by the ZMCC from the northern regions.

4.2.2 *Sand sources and transport processes*

The sandy sediments of SMT-Beaches along the SE China coast are mainly derived from the surrounding mountain rivers, weathering of bed rocks in both the Chinese mainland and islands, and erosion of the "Old Red Sand" and "Red Soil Platform". According to previous studies on heavy minerals, magnetic minerals, and geochemical compositions, the sandy particles of sediments collected from coastal areas of SE China are characterized by short transport distances (References in Table 3). In view of the contrasting sedimentary and morphological features between estuarine and bay SMT-Beaches (Zhao et al., 2020a, 2020b), their sandy sediment sources could also be different. The widespread small to mesoscale mountain rivers along the western coast of the TS, including the Minjiang River, Jiulong River, Jinjiang River, Jiaojiang River, Mulan River, and Zhangjiang River, provide important sediment sources for these well-developed SMT-Beaches in/near river estuaries (Wang and Ma, 1987; Yan, 1988; Hong, 1993; Chen et al., 1994; Xu, 1995, 1996; Hong and Chen, 2003; Fang et al., 2010, 2012; Ma et al., 2018). Otherwise, for SMT-Beaches located in semi-enclosed bays with limited sediment supplies, the erosion products of bedrock, "Old Red Sand", and "Red Soil Platform" under long-term warm and humid climatic conditions provide the majority of the sandy sediments (Chen, 1992; Chen and Guo, 1994; Gu et al., 2003; Xu et al., 2004; Yang and Wang, 2009; Hong, 2008; Zhang et al., 2008; Su et al., 2018). Furthermore, the stable sandy bodies and/or shallow sandy flats in the coastal areas can also contribute some sandy sediments to these SMT-Beaches under landward waves and/or currents.

The sandy sediments of SMT-Beaches along the SE China coast from various sources are under differential transport processes but are mainly hindered by both the ZMCC and the TWC and then deposited in coastal areas. These river-sourced sandy sediments are delivered by fresh water into the ocean and then dispersed under the influence of waves and tides. Simultaneously, the erosion products of bedrock from the Chinese main-

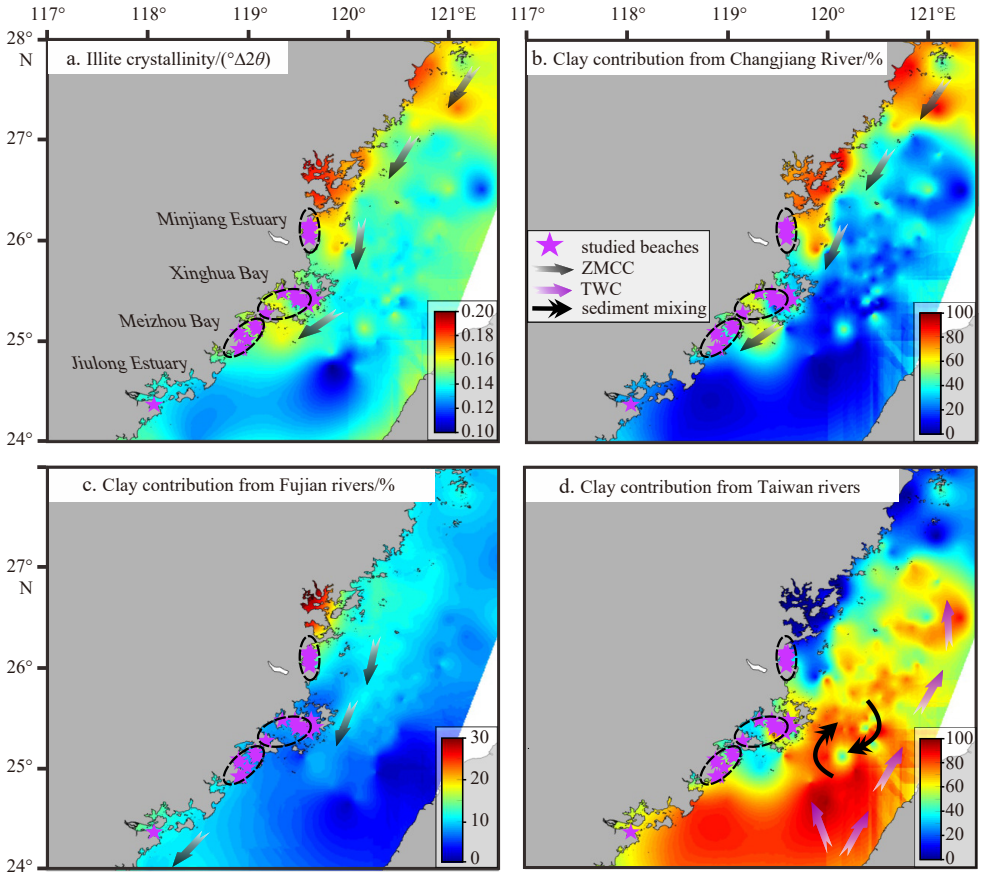

Fig. 6. Clay mineral contributions from various source regions. The spatial distribution of illite crystallinity in the Taiwan Strait (a); the spatial distribution of clay mineral contributions from the Changjiang River, Fujian rivers, and Taiwan rivers, respectively (b–d). ZMCC: Zhe-Min Coastal Current; TWC: Taiwan Warm Current.

land and islands are mainly carried out to the ocean by rainfall-induced water flows, while the "Old Red Sand" and "Red Soil Platform" are eroded and collapse under waves and coastal currents and are then brought into the ocean, providing another sediment source for SMT-Beaches. Nevertheless, all of these sandy particles are hindered by both the ZMCC and the TWC and are further constrained to be deposited in river estuaries and semi-enclosed bays (Yan, 1988; Chen, 1992, 1993; Xu, 1994, 1995; Horng and Huh, 2011; Fang et al., 2012; Chen et al., 2018; Ma et al., 2018; Li et al., 2019).

4.3 *SMT-Beach morphological responses to the decreased sediment supply*

Sufficient sediment supplies provide the basic material basis for SMT-Beach evolution along the SE China coast. According to the above discussion, the muddy sediments of these SMT-Beaches are sourced mainly from Fujian rivers and the Changjiang River (including a minor proportion from Zhejiang rivers), while the sandy sediments originate mostly from Fujian rivers and the erosion products of nearby regions. Despite the potentially different sandy sediment sources between estuarine and bay SMT-Beaches, the much wider mudflat section than sandy section of each SMT-Beach (Zhao et al., 2020a, b) indicates that riverine fine sediments are quite important. Consequently, changes in the sediment discharge of rivers could play a key role in the morphological evolution of SMT-Beaches.

For these estuarine SMT-Beaches along the SE China coast, the observed decreases in their sandy section width mainly correlate with reduced sediment supplies (Figs 7a, b) associated with decreased sediment discharges of mountain rivers surrounding the TS under extensive human activities (Walling, 2006; Syvitski et al., 2009). Most beaches along the Chinese mainland coast developed during the high sea-level period following the last transgression in the mid-Holocene (~6.0–5.5 ka BP) (Lei et al., 2014; Cai, 2019), which is closely associated with sufficient sediment supplies from tremendously small rivers to world large rivers. However, dramatic decreases in river sediment discharges all over the world under extensive and increasing human activities (such as dam construction, river sand mining, conservation of water and soil, and anthropogenic river walls) (Walling, 2006; Syvitski et al., 2009; Milliman and Farnsworth, 2011; Wu et al., 2020) have greatly reduced sediment supplies to coastal beaches, and this is especially obvious for these estuarine SMT-Beaches along the SE China coast. As the main sediment suppliers, the large decreases in the fluvial sediment discharges of both the Minjiang River and Changjiang River since the 1990s have resulted in an imbalance between the sediment budget and hydrodynamics, leading to obvious erosion in river deltas and adjacent coastal regions (Figs 7c, d, and 8a; MWRC, 2002–2020; Chen et al., 2010; Yang et al., 2011; Gao et al., 2019). As the sediment discharge decrease in the Minjiang River was mainly due to dam construction, the sandy sediment sources of SMT-Beaches have greatly decreased, resulting in landward SMT migration coupled with sandy section width reductions (Fig. 8b). Based on time series remote sensing images, the sandy section width of Longsha Beach in the Minjiang Estuary was reduced by 10 m from

Table 3. A compilation of previous investigations on sandy sediment sources in the western Taiwan Strait

No.	Region	Method	Numbers of samples	Reference
1	Sansha Bay	heavy minerals	91	Hong (2008)
2	Minjiang River	heavy minerals	9	Chen et al. (2018)
			20	Ma et al. (2018)
3	Minjiang Estuary	detrital minerals	230	Ma et al. (2018)
			60	Yan (1988)
			27	Xu (1995, 1996)
			7	Xu (1996)
4	Xinghua Bay	heavy minerals	17	Xu et al. (2004)
		major and trace elements & rare earth elements	93	Su et al. (2018)
5	Meizhou Bay	detrital minerals	/	Chen (1992)
6	Quanzhou Bay	detrital minerals	13	Gu et al. (2003)
7	Jiulong Estuary	detrital minerals	153	Chen et al. (1994)
			13	Xu (1994)
			40	Hong and Chen (2003)
		rare earth elements	15	Jin et al. (2010)
8	Xiamen Bay	detrital minerals	126	Wang and Ma (1987)
			127	Hong (1993)
			35	Fang et al. (2010)
9	Dongshan Bay	heavy minerals	132	Chen and Guo (1994)
10	Taiwan Strait	cetrital minerals	206	Chen (1993)
			68	Fang et al. (2012)
			150	Ma et al. (2018)
			26	Shen et al. (2021)
		magnetic minerals	241	Horng and Huh (2011)
			228	Yang and Wang (2009)
		major and trace elements	1 172	Li et al. (2019)

Note: "/" means the sample amounts are not present in the publication.

2004 to 2020 (Figs 7a, b). Additionally, the decreased sediment supply led to the obvious retreat/erosion of sandy beaches in the study area, with a minor portion of sandy beaches becoming SMT-Beaches (Liu et al., 2011; Cai, 2019).

Simultaneously, for these bay SMT-Beaches along the SE China coast, the decreases in their sandy sediment sources are mainly correlated with human activities, such as hard seawall construction, coastal reclamation, and sand mining, resulting in sandy sections with reduced widths (Figs 7e–h). Solid seawalls and coastal reclamation have hindered transport of the erosion product of bedrock, "Old Red Sand", and "Red Soil Platform" to coastal beaches, while coastal sand mining and/or sand stealing have also reduced their sandy sediment sources. According to time series images, the sandy section width of Yulou Beach in Fuqing Bay decreased by 1–3 m from 2009 to 2017 (Figs 7e, f), while that of Lieyu Beach in Dongshan Bay decreased by 3–5 m from 2008 to 2019 (Figs 7g, h). In particular, these observations have also been confirmed by personal communications with many local people and viewed by the landward SMT migration of Jingfeng Beach in Meizhou Bay and Jiangyin East Beach in Xinghua Bay (Liu et al., 2011; Zhao et al., 2020b).

By comparison, the muddy sediment sources of all SMT-Beaches along the SE China coast present temporarily limited changes, and the mudflats of SMT-Beaches are mainly stable or are even expanding. This trend means that the SMT boundaries of SMT-Beaches are migrating landward and reducing the widths of their upper sandy sections, leading to the retreat of SMT-Beaches. During past decades, sediment discharges of Chinese mainland rivers have largely decreased (MWRC, 2002–2020; Wu et al., 2020; Figs 7c, d), while the transport capacity of the ZMCC has likely been reduced synchronously, mainly due to the weakened East Asian winter monsoon (D'Arrigo et al., 2005). However, the muddy sediments delivered to the SE China coast are not clearly decreasing, and the sedimentation rate along the northern coasts of the study region has even increased to a certain degree (Gao et al., 2019). These observations are mainly correlated with the rapid source-to-sink transfer between the Changjiang River and its subaqueous delta under intensive human activities. In response to thousands of dam proliferations, the sediment discharge of the Changjiang River was greatly reduced from ~470 Mt/a in the 1950s to ~110 Mt/a after the construction of the Three Gorges Dam (the world's largest dam; Yang et al., 2011; Dai and Liu, 2013; Dai et al., 2016; Dai, 2021), leading to strong erosion of its mid-lower riverbed, river catchment, coastal areas, subaqueous delta, and its distal muddy deposits (Yang et al., 2011, 2018; Dai et al., 2018; Gao et al., 2019). Then, these eroded regions with coarsened grain-sizes in both the suspended and surface sediments were converted into sediment source areas, e.g., the previous sinks like middle-lower riverbed and shoals in the estuarine channels have now become sediment sources (Dai et al., 2018), providing sufficient sediments to maintain the stability and/or expansion of Zhe-Min coastal mudflats (Gao et al., 2019), even the largely decreased sediment supply of the Changjiang River including Zhejiang and Fujian rivers. Simultaneously, the weakened East Asian winter monsoon could reduce the wave height along coastal areas (Chien et al., 2014), resulting in relatively more fine sediment deposition and maintenance of the stability and/or expansion of the studied SMT-Beach mudflats. Nevertheless, due to the decreasing sediment supply of rivers undergoing long-term "starvation", the eroded sediments from the mid-lower riverbed, delta and distal muds cannot provide sufficient sediments to support widespread mud-

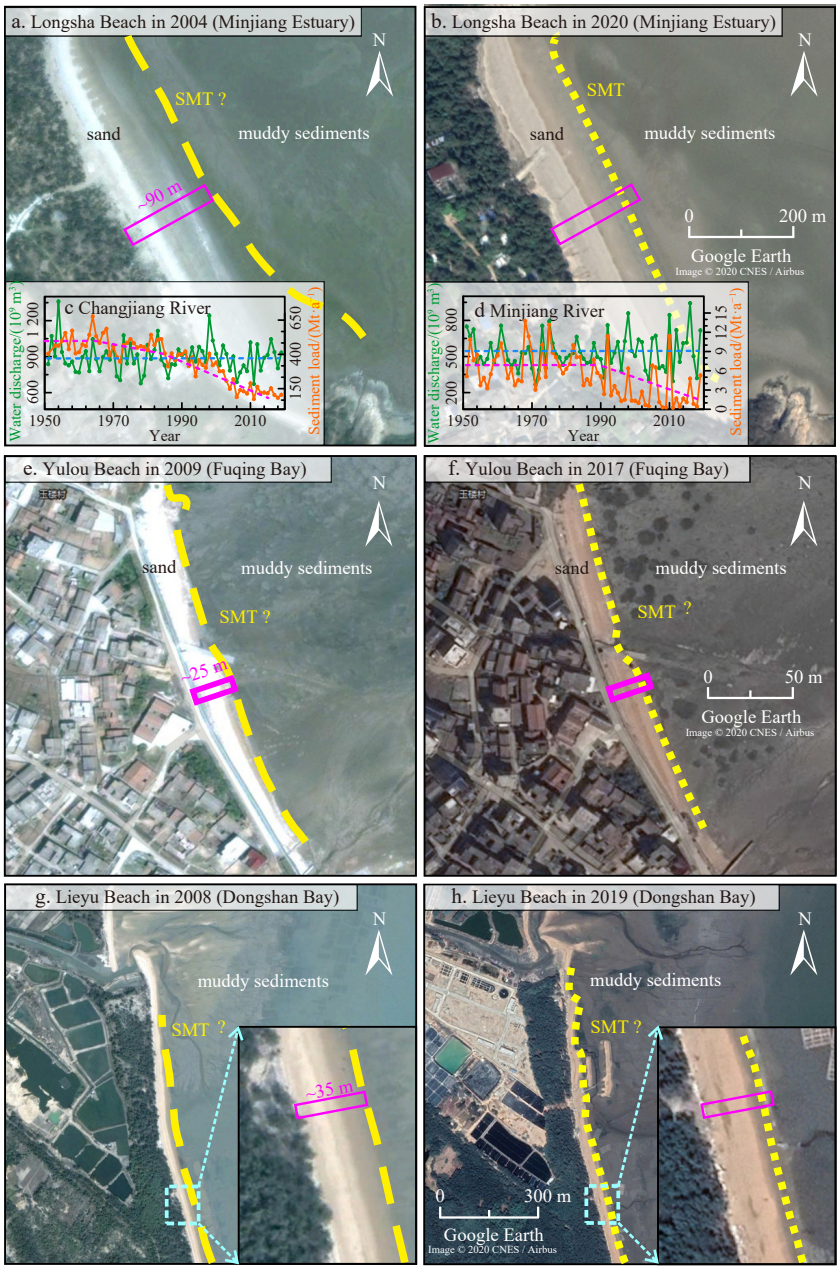

Fig. 7. Morphological changes in SMT-Beaches along the southeastern China coast inferred from Google Earth images. a–b, e–f, and g–h present Longsha Beach in the Minjiang Estuary from 2004 to 2020, Yulou Beach in Fuqing Bay from 2009 to 2017, and Lieyu Beach in Dongshan Bay from 2008 to 2019, respectively. c–d indicate both the water and fluvial sediment discharges of the Changjiang River and Minjiang River, respectively (MWRC, 2002–2020). The yellow dotted and dashed lines represent the overall SMT distribution of SMT-Beaches inferred from the delineation of Zhao et al. (2020b); the dotted line in b refers to Zhao et al. (2020a). The lengths of the longer sides of the bright purple rectangles show the sandy section widths of the above three beaches in 2004, 2009, and 2008, indicating decreasing sandy section widths with clear landward SMT migration.

flat stability or expansion along the SE China coast. Consequently, when the erosion-deduced sediment supplies for mudflats reach a threshold value, SMT-Beaches are expected to retreat due to insufficient sediment sources in the future.

Furthermore, the stability and development of SMT-Beaches are also closely correlated with global climate changes and other human activities, which tend to reduce the widths of the upper sandy sections. In view of global warming, sea-level rise, and increases in both the frequency and strength of tropical typhoons and winter storms, the erosion of coastal beaches is increasingly difficult to recover (Masselink et al., 2016; Luijendijk et al., 2018; Mentaschi et al., 2018; Vousdoukas et al., 2020). Particularly, under such an obviously decreasing sediment supply, the coastal regions of SE China are suffering 1.5–2.0 typhoons every year (Wang, 2004; Chien et al., 2014), resulting in the clear erosion of coastal beaches near typhoon-loading areas. Simultaneously, the sea-level rise along the coast of China has reached a value of 3.4 mm/a, while the local sea-level along the SE China coast is expected to rise with values of 65–160 mm during the next three decades (MNRC, 2021), tending toward widespread beach retreat, according to the Bruun Rule. Additionally, some beaches also suffer from sand stealing, anthropogenic pollution, and

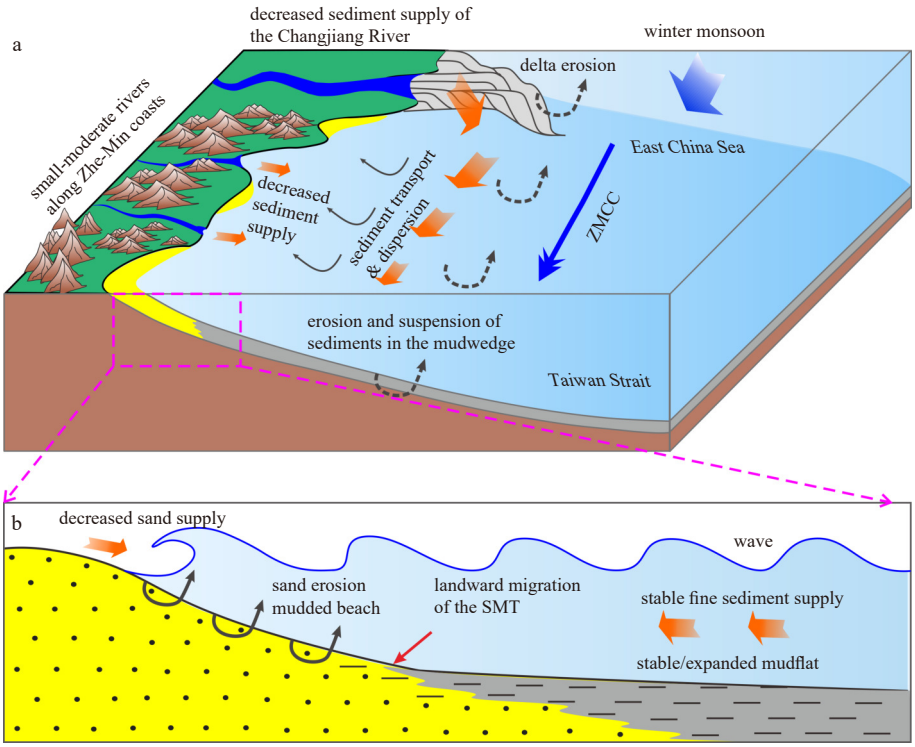

Fig. 8. Morphological responses of SMT-Beach to sediment source changes along the southeastern China coast. Sediment source-to-sink transport processes of SMT-Beaches in the study area (a); the potential responses of SMT-Beach morphology to decreases in river sediment supply (b).

weakened hydrodynamics under coastal engineering, leading to obvious changes in their sediment source-to-sink processes (Mao et al, 2007; Fu and Liu, 2016; Huang et al., 2016; Zhang et al., 2017; Gong, 2019). The resulting sandy sediment supply decreases coupled with increasing muddy sediment supplies could further lead to coastal beach retreat with landward SMT migration.

To summarize, according to the sediment source-to-sink process analysis conducted in this study, the morphological evolution of SMT-Beaches indicates close correlations with sediment discharge variations in both small-moderate mountain rivers and the Changjiang River (Fig. 8). Most SMT-Beaches along the SE China coast present an overall muddying tendency characterized by landward SMT migration. The upper sandy sections are narrowing along with decreasing sandy sediment sources, while the lower mudflats indicate relative stability or even expansion associated with sufficient muddy sediment supplies at present (Fig. 8b). Despite these findings, the sand-mud interaction mechanism present during the morphological changes in SMT-Beaches is still unclear, and future studies analyzing in situ observations over various time scales are required to better address the issues associated with SMT-Beach morphological evolution and muddying processes, as well as the potential controlling factors.

5 Conclusions

The clay mineralogy of surface sediments from SMT-Beaches and surrounding mountain rivers and semi-enclosed bays along the coast of southeastern China was investigated to constrain SMT-Beach sediment source-to-sink processes and their morphological indications. The following conclusions were obtained in this study.

(1) The clay minerals of SMT-Beaches are mainly composed of dominant kaolinite (15%–66%) and moderate illite (12%–38%), chlorite (10%–28%), and smectite (1%–32%) contents. From surrounding mountain rivers to SMT-Beaches, the clay mineral assemblages show distinct spatial changes characterized by large decreases in kaolinite, while illite and smectite present relative increases.

(2) The muddy sediments of SMT-Beaches are mainly sourced from nearby mountain rivers and long-term transport from the Changjiang River. The sandy sediments of these beaches are mainly sourced from nearby mountain rivers, the weathering products of surrounding rocks on both the Chinese mainland and islands, and erosion of the “Old Red Sand” and “Red Soil Platform”.

(3) The morphological processes of SMT-Beaches are closely correlated to the sediment supplies of surrounding mountain rivers and the distal Changjiang River. Under decreased sediment discharges and intensive human activities, the sandy sections of SMT-Beaches mainly present clear erosion trends, whereas the muddy sediment supplies of SMT-Beaches are temporarily stable and relatively constant, resulting in the landward migration of the mudflats with relative transgression or accumulation.

Acknowledgements

We would like to thank Haitao Xu, Xiang Zhou, Chengtao Wang, and Jixiang Zheng from the Third Institute of Oceanography, MNR for their cooperation in collecting sediments. Yanli Li, Yijie Wang, and Xuan Lv from the State Key Laboratory of Marine Geology, Tongji University are thanked for their help with the laboratory analysis.

References

Aagaard T, Greenwood B, Hughes M. 2013. Sediment transport on

dissipative, intermediate and reflective beaches. Earth-Science Reviews, 124: 32–50, doi: 10.1016/j.earscirev.2013.05.002
Anthony E J, Gardel A, Dolique F, et al. 2002. Short-term changes in the plan shape of a sandy beach in response to sheltering by a nearshore mud bank, Cayenne, French Guiana. Earth Surface Processes and Landforms, 27(8): 857–866, doi: 10.1002/esp.357
Anthony E J, Gardel A, Dolique F, et al. 2015. Mud banks, sand flux and beach morphodynamics: Montjoly Lagoon Beach, French Guiana. In: Maanan M, Robin M, eds. Sediment Fluxes in Coastal Areas. Dordrecht: Springer, 75–90
Biscaye P E. 1965. Mineralogy and sedimentation of recent deep-sea clay in the Atlantic Ocean and adjacent seas and oceans. Geological Society of America Bulletin, 76(7): 803–832, doi: 10.1130/0016-7606(1965)76[803:MASORD]2.0.CO;2
Cai Feng. 2015. Chinese Beach Nourishment Manual (in Chinese). Beijing: China Ocean Press
Cai Feng. 2019. Brief Introduction of Chinese Beach Resources (in Chinese). Beijing: China Ocean Press
Carranza-Edwards A, Kasper-Zubillaga J J, Martínez-Serrano R G, et al. 2019. Provenance inferred through modern beach sands from the Gulf of Tehuantepec, Mexico. Geological Journal, 54(1): 552–563, doi: 10.1002/gj.3205
Chang T S, Ha H J, Hong S H. 2016. Mud deposition on a Macrotidal Beach: Dasari coastal dune, West Coast of Korea. Journal of Coastal Research, 75(S1): 1312–1316
Chang T S, Hong S H, Chun S S, et al. 2017. Age and morphodynamics of a sandy beach fronted by a macrotidal mud flat along the west coast of Korea: a lateral headland bypass model for beach-dune formation. Geo-Marine Letters, 37(4): 361–371, doi: 10.1007/s00367-016-0486-y
Chen Huazhou. 1992. Assemblages and distribution characteristics of heavy minerals in Meizhou Bay. Journal of Oceanography in Taiwan Strait (in Chinese), 11(3): 211–217
Chen Huazhou. 1993. Characteristics and sources of heavy minerals in surface sediment of Taiwan Strait. Journal of Oceanography in Taiwan Strait (in Chinese), 12(2): 136–144
Chen Huazhou, Guo Yunmou. 1994. The composition and material sources of heavy minerals in Dongshan Bay and their environment meaning. Marine Sciences (in Chinese), (2): 40–44
Chen Huazhou, Guo Yumou, Yang Shunliang. 1994. Removal of heavy minerals in Jiulong River Estuary and its effect on the siltation in the south part of Xiamen west harbour. Tropic Oceanology (in Chinese), 13(1): 39–46
Chen Xinyi, Huang Chi-Yue, Shao Lei. 2018. Characteristics of heavy minerals in modern sediments of Minjiang and Jiulongjiang Rivers, Fujian Province and their provenance implication. Journal of Palaeogeography (in Chinese), 20(4): 637–650
Chen Jing, Ma Junqiang, Xu Kehui, et al. 2017. Provenance discrimination of the clay sediment in the western Taiwan Strait and its implication for coastal current variability during the late-Holocene. The Holocene, 27(1): 110–121, doi: 10.1177/0959683616652706
Chen Jian, Yu Xingguang, Li Dongyi, et al. 2010. Characteristics of underwater morphology evolution of the Minjiang Estuary in recent 100 years and its reasons. The Ocean Engineering (in Chinese), 28(2): 82–89
Chien Hwa, Cheng Hao-Yuan, Chiou Ming-Da. 2014. Wave climate variability of Taiwan waters. Journal of Oceanography, 70(2): 133–152, doi: 10.1007/s10872-014-0218-8
Dai Zhijun. 2021. Changjiang Riverine and Estuarine Hydro-Morphodynamic Processes: In the Context of Anthropocene Era. Singapore: Springer
Dai Zhijun, Fagherazzi S, Mei Xuefei, et al. 2016. Decline in suspended sediment concentration delivered by the Changjiang (Yangtze) River into the East China Sea between 1956 and 2013. Geomorphology, 268: 123–132, doi: 10.1016/j.geomorph.2016.06.009
Dai Zhijun, Liu James T. 2013. Impacts of large dams on downstream fluvial sedimentation: An example of the Three Gorges Dam (TGD) on the Changjiang (Yangtze River). Journal of Hydrology, 480: 10–18, doi: 10.1016/j.jhydrol.2012.12.003
Dai Zhijun, Mei Xuefei, Darby S E, et al. 2018. Fluvial sediment transfer in the Changjiang (Yangtze) river-estuary depositional system. Journal of Hydrology, 566: 719–734, doi: 10.1016/j.jhydrol.2018.09.019
D'Arrigo R, Jacoby G, Wilson R, et al. 2005. A reconstructed Siberian High index since A. D. 1599 from Eurasian and North American tree rings. Geophysical Research Letters, 32(5): L05705
Fang Jianyong, Chen Jian, Li Yunhai, et al. 2010. Study of modern sedimentary environment in the Xiamen Bay. Acta Sedimentologica Sinica (in Chinese), 28(2): 356–364
Fang Jianyong, Chen Jian, Wang Aijun, et al. 2012. The distribution characteristics of grain size and mineral of surface sediment in the Taiwan Strait. Haiyang Xuebao (in Chinese), 34(5): 91–99
Fang Jianyong, Liu Zhifei, Zhao Yulong. 2018. High-resolution clay mineral assemblages in the inner shelf mud wedge of the East China Sea during the Holocene: Implications for the East Asian Monsoon evolution. Science China Earth Sciences, 61(9): 1316–1329, doi: 10.1007/s11430-017-9208-1
Flemming B. 2020. Beach sand and its origins. In: Jackson D W T, Short A D, eds. Sandy Beach Morphodynamics. Amsterdam: Elsevier, 15–37
Fu Boxin, Liu Lin. 2016. Beach mudding comprehensive regulation of Nantaiwu in Zhangzhou. Port & Waterway Engineering (in Chinese), (10): 50–56
Fu Xiang, Wu Shaohua, Li Tao, et al. 2013. Characteristics analysis of tide along Fujian mid-south coastal waters. Journal of Applied Oceanography (in Chinese), 32(2): 164–170
Gao Jianhua, Shi Yong, Sheng Hui, et al. 2019. Rapid response of the Changjiang (Yangtze) River and East China Sea source-to-sink conveying system to human induced catchment perturbations. Marine Geology, 414: 1–17, doi: 10.1016/j.margeo.2019.05.003
Gibbs R J. 1977. Clay mineral segregation in the marine environment. Journal of Sedimentary Research, 47(1): 237–243
Gong Yumeng. 2019. Research on restoration of muddy sand beach (in Chinese) [dissertation]. Hangzhou: Zhejiang University
Gu Dongqi, Bian Shuhua, Hu Zejian, et al. 2003. Distribution characteristics of mineral detritus in surface sediment from the Quanzhou Bay and their environmental significance. Coastal Engineering (in Chinese), 22(2): 22–30
Guo Junli, Shi Lianqiang, Chen Shenliang, et al. 2021. Sand-mud transition dynamics at embayed beaches during a typhoon season in eastern China. Marine Geology, 441: 106633, doi: 10.1016/j.margeo.2021.106633
He Mengying, Zheng Hongbo, Huang Xiangtong, et al. 2013. Yangtze River sediments from source to sink traced with clay mineralogy. Journal of Asian Earth Sciences, 69: 60–69, doi: 10.1016/j.jseaes.2012.10.001
Hein J R, Mizell K, Barnard P L. 2013. Sand sources and transport pathways for the San Francisco Bay coastal system, based on X-ray diffraction mineralogy. Marine Geology, 345: 154–169, doi: 10.1016/j.margeo.2013.04.003
Hong Huiliang. 1993. Research on heavy minerals in Xiamen Port. Haiyang Xuebao (in Chinese), 15(3): 49–62
Hong Huiliang. 2008. A study of heavy minerals in Sansha Bay. Journal of Oceanography in Taiwan Strait (in Chinese), 27(3): 381–392
Hong Huiliang, Chen Feng. 2003. Characteristics of heavy minerals in a core from Jiulongjiang Estuary. Journal of Oceanography in Taiwan Strait (in Chinese), 22(1): 65–78
Horng Chorng-Shern, Huh Chih-An. 2011. Magnetic properties as tracers for source-to-sink dispersal of sediments: A case study in the Taiwan Strait. Earth and Planetary Science Letters, 309(1–2): 141–152
Houston J R. 2013. The economic value of beaches. Shore & Beach, 81(4): 4–11
Huang Shichang, Yao Wenwei, Liu Xu, et al. 2016. Profile characteristics of the beaches adjacent to muddy seabed in the headland bays. Coastal Engineering (in Chinese), 35(4): 1–9
Jia Jiajun, Gao Jianhua, Cai Tinglu, et al. 2018. Sediment accumulation and retention of the Changjiang (Yangtze River) subaqueous delta and its distal muds over the last century. Marine

Geology, 401: 2–16, doi: 10.1016/j.margeo.2018.04.005
Jiang Chenghao, Shi Lianqiang, Cheng Lin, et al. 2014. The quality evaluation system of island beaches in Zhejiang and its application research. Journal of Marine Sciences (in Chinese), 32(1): 56–63
Jin Guie, Hong Xiaoyan, Wang Xiaxia, et al. 2010. Geochemical characteristics of rare earth elements in Jiulongjiang Estuary. Journal of Oceanography in Taiwan Strait (in Chinese), 29(3): 304–313
Komar P D. 1998. Beach Processes and Sedimentation. 2nd ed. New Jersey: Prentice Hall
Lei Gang, Cai Feng, Su Xianze, et al. 2014. Tectonic geneses of regional differential distribution and accumulated morphology of Chinese sandy beaches. Journal of Applied Oceanography (in Chinese), 33(1): 1–10
Li Tao, Cai Guanqiang, Wang Chaowen, et al. 2021. Quantifying clay mineral sources in marine sediments by using end-member mixing analysis. Geo-Marine Letters, 41(1): 6, doi: 10.1007/s00367-020-00674-4
Li Tao, Sun Guihua, Yang Chupeng, et al. 2019. Source apportionment and source-to-sink transport of major and trace elements in coastal sediments: Combining positive matrix factorization and sediment trend analysis. Science of the Total Environment, 651: 344–356, doi: 10.1016/j.scitotenv.2018.09.198
Liu Jianhui, Cai Feng, Qi Hongshuai, et al. 2011. Coastal erosion along the west coast of the Taiwan Strait and it's influencing factors. Journal of Ocean University of China, 10(1): 23–34, doi: 10.1007/s11802-011-1745-1
Liu Jianguo, Cao Li, Yan Wen, et al. 2019. New archive of another significant potential sediment source in the South China Sea. Marine Geology, 410: 16–21, doi: 10.1016/j.margeo.2019.01.003
Liu Zhifei, Colin C, Huang Wei, et al. 2007b. Clay minerals in surface sediments of the Pearl River drainage basin and their contribution to the South China Sea. Chinese Science Bulletin, 52(8): 1101–1111, doi: 10.1007/s11434-007-0161-9
Liu Xiting, Li Anchun, Dong Jiang, et al. 2018. Provenance discrimination of sediments in the Zhejiang-Fujian mud belt, East China Sea: Implications for the development of the mud depocenter. Journal of Asian Earth Sciences, 151: 1–15, doi: 10.1016/j.jseaes.2017.10.017
Liu J P, Liu C S, Xu Kehui, et al. 2008a. Flux and fate of small mountainous rivers derived sediments into the Taiwan Strait. Marine Geology, 256(1–4): 65–76
Liu Zhifei, Tuo Shouting, Colin C, et al. 2008b. Detrital fine-grained sediment contribution from Taiwan to the northern South China Sea and its relation to regional ocean circulation. Marine Geology, 255(3–4): 149–155
Liu J P, Xu Kehui, Li Anchun, et al. 2007a. Flux and fate of Yangtze River sediment delivered to the East China Sea. Geomorphology, 85(3–4): 208–224
Liu Zhifei, Zhao Yulong, Colin C, et al. 2016. Source-to-sink transport processes of fluvial sediments in the South China Sea. Earth-Science Reviews, 153: 238–273, doi: 10.1016/j.earscirev.2015.08.005
Luijendijk A, Hagenaars G, Ranasinghe R, et al. 2018. Author Correction: The State of the World's Beaches. Scientific Reports, 8: 11381, doi: 10.1038/s41598-018-28915-8
Ma Xiaohong, Han Zongzhu, Zhang Yong, et al. 2018. Heavy minerals in shelf sediments off Fujian-Zhejiang coast of the East China Sea: Their provenance and geological application. Journal of Ocean University of China, 17(6): 1369–1381, doi: 10.1007/s11802-018-3754-9
Mao Longjiang, Zhang Yongzhan, Zhang Zhenke, et al. 2007. Characteristics of sedimentary environments in Sanya Bay of Hainan Island. Marine Geology & Quaternary Geology (in Chinese), 27(4): 17–22
Masselink G, Castelle B, Scott T, et al. 2016. Extreme wave activity during 2013/2014 winter and morphological impacts along the Atlantic coast of Europe. Geophysical Research Letters, 43(5): 2135–2143, doi: 10.1002/2015GL067492
Mehring J L, McBride E F. 2007. Origin of modern quartzarenite beach sands in a temperate climate, Florida and Alabama, USA. Sedimentary Geology, 201(3–4): 432–445
Mentaschi L, Vousdoukas M I, Pekel J F, et al. 2018. Global long-term observations of coastal erosion and accretion. Scientific Reports, 8(1): 12876, doi: 10.1038/s41598-018-30904-w
Milliman J D, Farnsworth K L. 2011. River Discharge to the Coastal Ocean: A Global Synthesis. Cambridge: Cambridge University Press, 2–163
Ministry of Natural Resources of China (MNRC). 2019–2021. Statistical Bulletin of China Marine Economy (in Chinese). Beijing: Ministry of Natural Resources
Ministry of Natural Resources of China (MNRC). 2021. Statistical Bulletin of China Sea Level (in Chinese). Beijing: Ministry of Natural Resources
Ministry of Water Resource of China (MWRC). 2002–2020. China River Sediment Bulletin (in Chinese). Beijing: China Water & Power Press
Morio O, Sedrati M, Goubert E, et al. 2016. Morphodynamic of a sandy-muddy macrotidal estuarine beach under contrasted energy conditions (Vilaine Estuary, France). Journal of Coastal Research, 75(S1): 258–262
Morrone C, Le Pera E, Marsaglia K M, et al. 2020. Compositional and textural study of modern beach sands in the active volcanic area of the Campania region (southern Italy). Sedimentary Geology, 396: 105567, doi: 10.1016/j.sedgeo.2019.105567
Parra J G, Marsaglia K M, Rivera K S, et al. 2012. Provenance of sand on the Poverty Bay shelf, the link between source and sink sectors of the Waipaoa River sedimentary system. Sedimentary Geology, 280: 208–233, doi: 10.1016/j.sedgeo.2012.04.012
Pereira P S, Calliari L J, Holman R, et al. 2011. Video and field observations of wave attenuation in a muddy surf zone. Marine Geology, 279(1–4): 210–221
Shen Xiaotian, Jian Xing, Li Chao, et al. 2021. Submarine topography-related spatial variability of the southern Taiwan Strait sands (East Asia). Marine Geology, 436: 106495, doi: 10.1016/j.margeo.2021.106495
Short A D. 1991. Macro-meso tidal beach morphodynamics–An overview. Journal of Coastal Research, 7(2): 417–436
Short A D. 2006. Australian beach systems—nature and distribution. Journal of Coastal Research, 22(1): 11–27
Stronge W B. 2005. Economic value of beaches. In: Schwartz M L, ed. Encyclopedia of Coastal Science. Encyclopedia of Earth Science Series. Dordrecht: Springer
Su Ni, Bi Lei, Guo Yulong, et al. 2018. Rare earth element compositions and provenance implications: A case from sediments of the Mulanxi River Estuary and surrounding sea area. Marine Geology & Quaternary Geology (in Chinese), 38(1): 150–159
Syvitski J P M, Kettner A J, Overeem I, et al. 2009. Sinking deltas due to human activities. Nature Geoscience, 2(10): 681–686, doi: 10.1038/ngeo629
Syvitski J P M, Vörösmarty C J, Kettner A J, et al. 2005. Impact of humans on the flux of terrestrial sediment to the global coastal ocean. Science, 308: 376–380, doi: 10.1126/science.1109454
Tamura T, Horaguchi K, Saito Y, et al. 2010. Monsoon-influenced variations in morphology and sediment of a mesotidal beach on the Mekong River delta coast. Geomorphology, 116(1–2): 11–23
Vousdoukas M I, Ranasinghe R, Mentaschi L, et al. 2020. Sandy coastlines under threat of erosion. Nature Climate Change, 10(3): 260–263, doi: 10.1038/s41558-020-0697-0
Walling D E. 2006. Human impact on land–ocean sediment transfer by the world's rivers. Geomorphology, 79(3–4): 192–216
Wang Chuankun. 2004. Features of monsoon, typhoon and sea waves in the Taiwan Strait. Marine Georesources & Geotechnology, 22(3): 133–150
Wang Yongxun, Ma Wentong. 1987. Q-mode factor analysis of heavy minerals in the surface sediments in the Xiamen harbour. Journal of Oceanography in Taiwan Strait (in Chinese), 6(3): 214–220
Wilson M J. 2004. Weathering of the primary rock-forming minerals: processes, products and rates. Clay Minerals, 39(3): 233–266,

doi: 10.1180/0009855043930133
Wright L D, Short A D. 1984. Morphodynamic variability of surf zones and beaches: a synthesis. Marine Geology, 56(1–4): 93–118
Wu Ziyin, Zhao Dineng, Syvitski J P M, et al. 2020. Anthropogenic impacts on the decreasing sediment loads of nine major rivers in China, 1954–2015. Science of the Total Environment, 739: 139653, doi: 10.1016/j.scitotenv.2020.139653
Xu Dongyu. 1985. Mud sedimentation on the East China Sea continental shelf. Marine Geology & Quaternary Geology (in Chinese), 5(2): 17–26
Xu Kehui, Li Anchun, Liu J P, et al. 2012. Provenance, structure, and formation of the mud wedge along inner continental shelf of the East China Sea: a synthesis of the Yangtze dispersal system. Marine Geology, 291–294: 176–191
Xu Kehui, Milliman J D, Li Anchun, et al. 2009. Yangtze- and Taiwan-derived sediments on the inner shelf of East China Sea. Continental Shelf Research, 29(18): 2240–2256, doi: 10.1016/j.csr.2009.08.017
Xu Maoquan. 1994. Study on fragmentary minerals surface sediments in Jiulong River Estuary. Journal of Xiamen University (Natural Science) (in Chinese), 33(5): 675–680
Xu Maoquan. 1995. Studies on fragmentary minerals in surface sediments of the Minjiang Estuary. Journal of Xiamen University (Natural Science) (in Chinese), 34(3): 466–469
Xu Maoquan. 1996. Study on heavy minerals in surface sediments of Minjiang Estuary. Journal of Oceanography in Taiwan Strait (in Chinese), 15(3): 229–234
Xu Yonghang, Chen Jian, Wang Aijun, et al. 2013. Clay minerals in surface sediments of the Taiwan Strait and their provenance. Acta Sedimentologica Sinica (in Chinese), 31(1): 120–129
Xu Yonghang, Sun Qinqin, Yi Liang, et al. 2014. The source of natural and anthropogenic heavy metals in the sediments of the Minjiang River Estuary (SE China): Implications for historical pollution. Science of the Total Environment, 493: 729–736, doi: 10.1016/j.scitotenv.2014.06.046
Xu Maoquan, Xu Wenbin, Sun Meiqin, et al. 2004. The characteristics of heavy minerals composition and distribution in surface sediment from the Xinghua Bay of Fujian. Haiyang Xuebao (in Chinese), 26(5): 74–82
Yan Suzhuang. 1988. Characteristics of heavy minerals distribution in the surface sediments in Minjiang estuarine region. Journal of Oceanography in Taiwan Strait (in Chinese), 7(2): 112–118
Yang Zuosheng. 1988. Mineralogical Assemblages and chemical characteristics of clays from sediments of the Huanghe, Changjiang, Zhujiang rivers and their relationship to the climate environment in their sediment source areas. Oceanologia et Limnologia Sinica (in Chinese), 19(4): 336–346
Yang Zuosheng, Guo Zhigang, Wang Zhaoxiang, et al. 1992. Macro pattern of the suspension transport from the shelf of Yellow Sea and East China Sea to its eastern deep water region. Haiyang Xuebao (in Chinese), 14(2): 81–90
Yang Shouye, Jung H S, Lim D II, et al. 2003. A review on the provenance discrimination of sediments in the Yellow Sea. Earth-Science Reviews, 63(1–2): 93–120
Yang Shilun, Milliman J D, Li Ping, et al. 2011. 50, 000 dams later: Erosion of the Yangtze River and its delta. Global and Planetary Change, 75(1–2): 14–20
Yang Lijing, Wang Weiguo. 2009. Distribution characteristics of magnetic susceptibility of surficial sediments in the western Taiwan Strait. Acta Sedimentologica Sinica (in Chinese), 27(4): 697–703
Yang Haifei, Yang Shilun, Meng Yi, et al. 2018. Recent coarsening of sediments on the southern Yangtze subaqueous delta front: A response to river damming. Continental Shelf Research, 155: 45–51, doi: 10.1016/j.csr.2018.01.012
Zhang Chunhua, Liu Jingui, Yang Jing. 2017. Studies on muddy and consolidating process at Silver Beach in Beihai. Marine Forecasts (in Chinese), 34(6): 83–88
Zhang Jiafu, Yuan Baoyin, Zhou Liping. 2008. Luminescence chronology of "Old Red Sand" in Jinjiang and its implications for optical dating of sediments in South China. Chinese Science Bulletin, 53(4): 591–601, doi: 10.1007/s11434-008-0001-6
Zhao Shaohua, Cai Feng, Liu Zhifei, et al. 2021. Disturbed climate changes preserved in terrigenous sediments associated with anthropogenic activities during the last century in the Taiwan Strait, East Asia. Marine Geology, 437: 106499, doi: 10.1016/j.margeo.2021.106499
Zhao Shaohua, Cai Feng, Qi Hongshuai, et al. 2020a. Contrasting sand-mud transition migrations in estuarine and bay beaches and their potential morphological responses. Geomorphology, 365: 107243, doi: 10.1016/j.geomorph.2020.107243
Zhao Rui, Hynes S, He Guangshun. 2014. Defining and quantifying China's ocean economy. Marine Policy, 43: 164–173, doi: 10.1016/j.marpol.2013.05.008
Zhao Shaohua, Liu Zhifei, Colin C, et al. 2018a. Responses of the East Asian Summer monsoon in the low-latitude South China Sea to high-latitude millennial-scale climatic changes during the Last Glaciation: evidence from a high-resolution clay mineralogical record. Paleoceanography and Paleoclimatology, 33(7): 745–765, doi: 10.1029/2017PA003235
Zhao Shaohua, Qi Hongshuai, Cai Feng, et al. 2020b. Morphological and sedimentary features of sandy-muddy transitional beaches in estuaries and bays along mesotidal to macrotidal coasts. Earth Surface Processes and Landforms, 45(7): 1660–1676, doi: 10.1002/esp.4837
Zhao Yifei, Zou Xinqing, Gao Jianhua, et al. 2018b. Clay mineralogy and source-to-sink transport processes of Changjiang River sediments in the estuarine and inner shelf areas of the East China Sea. Journal of Asian Earth Sciences, 152: 91–102, doi: 10.1016/j.jseaes.2017.11.038
Zheng Wenzhen, Chen Funian, Chen Xinzhong. 1982. Tides and tidal currents in the Taiwan Strait. Journal of Oceanography in Taiwan Strait (in Chinese), 1(2): 1–4